



ELSEVIER

Available online at www.sciencedirect.com

ScienceDirect

journal homepage: www.elsevier.com/locate/he

Solid oxide carbonate composite fuel cells: Size effect on percolation

Shalima Shawuti*, Mehmet Ali Gülgün

Faculty of Engineering and Natural Science, Sabanci University, 34956, Istanbul, Turkey

ARTICLE INFO

Article history:

Received 5 May 2016

Received in revised form

17 July 2016

Accepted 23 July 2016

Available online 30 August 2016

Keywords:

Composite electrolyte

SOFC

Interface

Percolation

Carbonate

Impedance

ABSTRACT

In the studies of solid oxide carbonate composite fuel cell, percolation behaviour of the two phases was investigated as a function of particle size of the oxide phase. The ratio of amount of samarium doped ceria (SDC; $\text{Sm}_{0.2}\text{Ce}_{0.8}\text{O}$) to Na_2CO_3 was varied to determine an optimum ionic conductivity as function of oxide particle size. The roles of both phases in the composite electrolyte were investigated. SDC particles were mixed in different amounts of Na_2CO_3 to obtain composites with carbonate ratios from 1 wt% to 50 wt%. Micro-structural investigations showed that Na_2CO_3 phase served as the matrix in the micro-structure gluing the oxide particles together. The lowest and the highest carbonate ratios caused low conductivities in the composite as in these samples the 3D connectivity of both phases were disrupted. Low conductivity at both ends of the mixture composition could be interpreted as none of the components of the composite dominated the ionic conductivity. The highest conductivity was obtained at 10 wt% Na_2CO_3 amount in the composite electrolyte when nano-sized SDC (5–10 nm) oxide powders were used. Two different particle sizes of SDC powders were used to show that the optimum phase ratio, i.e. percolation of both phases, is function of particle size as well. The conductivity in the composite showed percolation behaviour with respect to the two constituent phases.

© 2016 Hydrogen Energy Publications LLC. Published by Elsevier Ltd. All rights reserved.

Introduction

Solid oxide fuel cells (SOFC) are regarded as a viable alternative energy conversion system for electrical power generation because of their high power efficiencies and tolerance to many different fuels [1,2]. In recent years, in order to achieve more competitive production and operating costs, investigations on solid oxide fuel cells (SOFCs) focussed onto the intermediate-temperature range (between 600 °C and 800 °C) electrolytes. Intermediate-temperature SOFCs, in general, or nano-composite fuel cell, in particular, have a potential for commercial scale production [3].

The performance of the electrolyte can be enhanced by reducing the electrolyte thickness and/or using alternative materials with high ionic conductivities [4]. Among these alternative materials, ceria based alkali carbonate composite electrolyte has an advantage of having a low activation energy for intermediate temperature range when compared to single phase oxide electrolytes like rare-earth doped ceria [5].

The composite electrolytes, in general, are composed of high ionic conductivity oxides, like SDC, coated with alkali salts (carbonate, chloride, hydrate, or sulphate) [6]. The literature on nano-composite electrolyte suggested that the oxide particles provided a skeleton for the composite at operating temperatures [7]. Furthermore, it was shown the electrolyte

* Corresponding author.

E-mail addresses: shalima@sabanciuniv.edu (S. Shawuti), m-gulgun@sabanciuniv.edu (M.A. Gülgün).

<http://dx.doi.org/10.1016/j.ijhydene.2016.07.208>

0360-3199/© 2016 Hydrogen Energy Publications LLC. Published by Elsevier Ltd. All rights reserved.

remains as a composite with two stable phases at operating temperatures [7]. Thus, composite electrolytes utilize the best properties of each component. Therefore, SDC based nano-composites appear to be a promising candidate for the low cost and high conductivity electrolytes [6].

In an SDC based nano-composites electrolyte, SDC phase acts as the oxygen ion conductor, whereas the carbonate matrix was reported as a multiple ion conductor [8–15]. Liu et al., reported that at a 20% weight ratio of Na_2CO_3 the conductivity value peaked at its highest total value of 0.01 S/cm at 481 °C [16]. On the other hand, Rahman et al., observed that the best thermal expansion compatibility with the electrodes was at 50% weight of Na_2CO_3 [17]. Work by Xia et al., showed that composite with 50 wt% carbonate reached 0.1 S cm^{-1} at 600 °C [18]. The average crystallite size of the SDC that was used in that study was 26 nm which was determined from XRD measurements using Scherrer's formula. The difference in the optimum Na_2CO_3 weight ratio appeared to be due to different particle/crystallite sizes of the oxide phase in these two studies [16,18].

The oxide/carbonate based nano-composite materials are very similar in their microstructure to a new class of liquid ionic conductors that attracted the attention as a promising candidate for ion batteries. The liquid ionic conductors consist of dispersed insulating solid oxide particles (e.g., SiO_2 , Al_2O_3 ... etc.) in the liquid non-aqueous lithium salt solutions (e.g., LiClO_4 in MeOH, THF... etc.) [19]. In these liquid electrolytes, the dependence of ionic conductivity on the oxide fraction showed a typical interfacial-percolation behaviour. The conductivities of the composite were low for very high or very low concentrations (ϕ) of the oxide particles (such as insulating silica nano-particles). The peak performance was achieved for intermediate concentrations where both phases of the composite were interconnected in 3D. In addition, for the concentrations with high conductivity, the composites revealed favourable mechanical properties of a soft materials similar to that of 'soggy sand' [20]. This viscous feature and the high conductivities make 'Soggy Sand' electrolytes useful in electrochemical devices such as rechargeable lithium batteries and Dye-Sensitized Solar Cells (DSSCs) [21,22].

In this research paper, ionic conductivity of nano-composite electrolyte prepared with two SDC powders with different particle sizes were investigated as a function of varied ratios of SDC filler particles to Na_2CO_3 matrix. An optimum ratio of carbonate to SDC was determined for the best ionic conductivity of the composite electrolyte. The investigations were also focused on the Na_2CO_3 percolation phenomena in the SDC- Na_2CO_3 composite.

Experimental procedures

Composite electrolytes with carbonate to oxide weight (wt %) ratios of 1, 5, 10, 15, 20, and 50 were prepared with SDC ($\text{Sm}_{0.2}\text{Ce}_{0.8}\text{O}_{1.9}$) powders (Fuel Cell Materials, Ohio, USA). Two SDC powders with different particle sizes were used. SDC powders labelled as HP had particle sizes from 0.1 to 0.4 μm with a measured specific surface area of 11 $\text{m}^2 \text{g}^{-1}$. SDC powders labelled as N20 had primary crystallite sizes from 5 to 10 nm with a measured specific surface area of 203 $\text{m}^2 \text{g}^{-1}$.

Na_2CO_3 anhydrous powders were purchased from Aldrich (Germany). The pellets were prepared by mixing weighted powders and dry ball-milling them in dry conditions for 6 h using 3 millimeter-sized YSZ (yttrium-stabilized zirconium) milling balls in HDPE bottles. The milled powders were collected and re-grounded manually in an agate mortar, before they were uniaxially pressed into 9 mm diameter and 1 mm thick pellets. They were then isostatically compressed under 40 MPa. The neat Na_2CO_3 and neat SDC pellets were also prepared through exactly the same procedure as the composites from pure commercial Na_2CO_3 and SDC powders. Then, Na_2CO_3 and SDC- Na_2CO_3 composite pellets were heat treated at 700 °C for 1 h under air atmosphere. The heating rate up to 700 °C was 5 °C min^{-1} . The pure SDC pellets were sintered at 1200 °C for 2 h in air.

Possible chemical reactions and phase distribution of the composites were monitored using X-ray diffraction (XRD) technique. The XRD patterns were recorded on a powder diffractometer with Cu K α radiation (1.5418 Å) in the 2 θ range of 10° and 90°. Microstructures of the sintered composites were investigated using a scanning electron microscope (FEG-SEM Leo Supra 35, Oberkochen, Germany) equipped with an energy dispersive x-ray spectrometer (EDS, Roentec, Berlin, Germany). A flash-dry silver paste (SPI Supplies, West Chester, USA) was painted on both surfaces of electrolyte pellets as contact electrodes covering the full top and bottom surfaces. The complex resistivity of the pellets were measured by a two-probe AC impedance spectrometer with an electrochemical interface (Solartron 1260 and 1286, respectively, Farnborough, UK), under an applied bias voltage with an amplitude of 100 mV AC. Electrochemical Impedance spectra (EIS) were recorded in the frequency range of 0.01 Hz–10 MHz from room temperature (RT) to 600 °C with a ProboStat™ cell (NorECs, Oslo, Norway) under air atmosphere. A parallel RC equivalent circuit was fitted to high frequency and low frequency data with the Z-View program. The total area of the silver electrodes was used in the conductivity calculations.

Results

The crystal structure of SDC composites with varied concentrations of Na_2CO_3 , 1 wt% (~5 vol%), 5 wt% (~12 vol%), 10 wt% (~23 vol%), 15 wt% (~32 vol%), 20wt% (~40 vol%) and 50 wt% (~73 vol%), were determined using the XRD patterns in Fig. 1. The XRD patterns of heat-treated (at 700 °C) composites with different amounts of Na_2CO_3 illustrated similar features. The XRD patterns in Fig. 1 were indexed employing JCPDS card no. 34-394 of crystalline CeO_2 with fluorite cubic structure. After annealing at 700 °C, no impurity or reaction phase, originating from SDC or Na_2CO_3 , was detected in the XRD patterns of composites with up to 50 wt% Na_2CO_3 concentrations. However, for composites with 50 wt% Na_2CO_3 , weak diffraction peaks were observed in the range of 2 θ values from 31° to 40°. The XRD patterns of as-received Na_2CO_3 and commercial Na_2CO_3 carbonate powders after heat-treatment at 700 °C were also shown in Fig. 1. On the XRD pattern of composite with 50 wt% Na_2CO_3 , several weak peaks at 2 θ values of 30.4°, 37.9°, and 40° were identified as crystalline peaks coming from

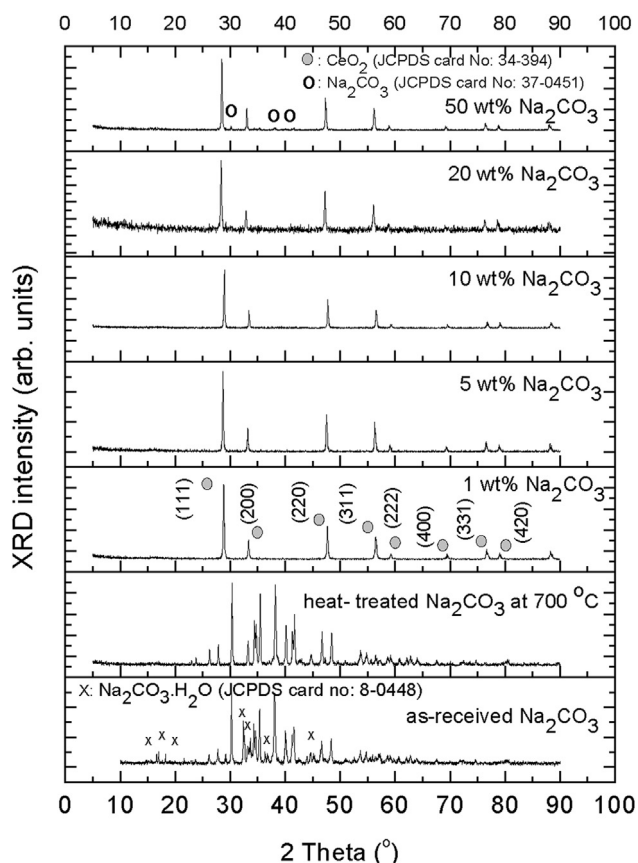


Fig. 1 – The room temperature XRD patterns of as-received and heat-treated (at 700 °C for 1 h) SDC (HP) composites with different Na₂CO₃ amounts, such as 1 wt%, 5 wt%, 10 wt%, 15 wt%, 20 wt%, and 50 wt%.

Na₂CO₃ with (JCPDS card no. 37-0451). On the other hand, only SDC peaks were detectable on the XRD plots of composite with 20 wt% Na₂CO₃. Having only SDC peaks in the XRD pattern of composite with 20 wt% Na₂CO₃ could be indicative that at least a portion of the Na₂CO₃ phase in the composites was not crystalline phase.

The diffraction pattern of as-received Na₂CO₃ powders also revealed peaks belonging to the hydrated sodium carbonate (Na₂CO₃·H₂O: i.e. monohydrate labelled with squares in Fig. 1). On the other hand, heat-treated powder (at 700 °C for 1 h) showed only peaks belonging to anhydrous sodium carbonate (Na₂CO₃). Anhydrous sodium carbonate is known to be hygroscopic. Unless precautions against moisture were taken, Na₂CO₃ absorbs water vapour readily and forms the monohydrate phase (Na₂CO₃·H₂O).

Fig. 2 shows the results of differential scanning calorimetry (DSC) analysis of heat-treated Na₂CO₃ pellet. The step change in baseline of the DSC response corresponding to the change in heat capacity is typical for a glass transition type reaction in an amorphous material [23]. Therefore, it could be indicative of a glass transition-like softening process of the partially amorphous Na₂CO₃ matrix.

The SEM morphologies of the composites with 1 wt%, 5 wt %, 10 wt%, 20 wt%, and 50 wt% carbonates are presented in Fig. 3. The micrograph of the composite with 1 wt%

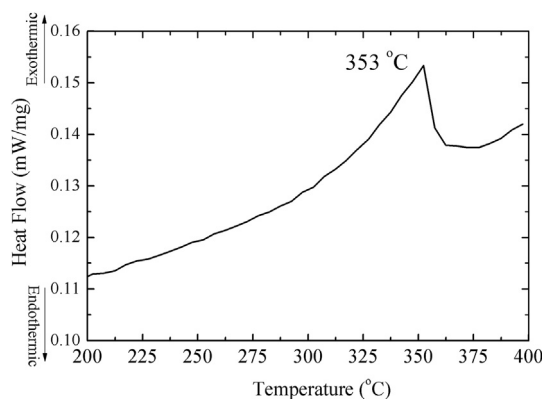


Fig. 2 – DSC analysis of heat-treated Na₂CO₃ pellet.

carbonate shows only the SDC particles without any carbonate phase. In the microstructure of 5 wt% composite two phases were imaged as separated and agglomerated regions. Two phases could be differentiated in the image by their contrast differences. The carbonate phase with a low average atomic number appeared as dark amorphous looking and featureless regions. A homogeneous and dense morphology was observed in the composite microstructure when 10 wt% carbonate concentration was used. With 20 wt% carbonate, inhomogeneous microstructures were obtained. The SEM image of composite containing 20 wt% Na₂CO₃ (Fig. 4) showed separated SDC particles in an over dominating Na₂CO₃ matrix. SDC oxide particles with high average atomic number appeared as isolated bright contrast agglomerates in a low average atomic number Na₂CO₃ matrix phase (appeared as dark contrast regions). In the micro-structure, the amorphous carbonate regions were dominant. In order to prove the carbonate phase in the micro-structure, EDS mapping of the 20 wt% of carbonate composite was also shown in Fig. 4. Highly concentrated Na elemental mapping was observed on the featureless dark region of Fig. 4. The samarium, ceria and sodium elemental mapping are overlapped on bright region.

Fig. 5a shows the impedance spectra of composites prepared with SDC (HP) powders with different carbonate amounts at 300 °C. The impedance spectrum of the SDC (HP) composite with 5 wt% Na₂CO₃ showed the lowest impedance resistivity value of $9.0 \times 10^4 \Omega \text{ cm}$. For the SDC composite with 1wt%, 10 wt%, 20 wt%, and 50 wt% Na₂CO₃, the impedance resistivity values were $1.9 \times 10^5 \Omega \text{ cm}$, $3.8 \times 10^5 \Omega \text{ cm}$, $1.1 \times 10^6 \Omega \text{ cm}$, and $1.0 \times 10^6 \Omega \text{ cm}$ respectively.

The effect of oxide particle size (i.e. which is related to different interface area between the carbonate matrix and the oxide particles) on the ionic conductivity were illustrated by Nyquist plots in Fig. 5b. Fig. 5b shows the impedance spectra of the composites prepared with nano-sized SDC (N20) powders. The impedance spectrum of the nano-sized SDC (N20) composite with 10 wt% Na₂CO₃ showed the lowest impedance resistivity values of $1.2 \times 10^5 \Omega \text{ cm}$. For the SDC composite with 1 wt%, 5 wt%, 20 wt%, and 50 wt% Na₂CO₃ the impedance resistivity values were $5.1 \times 10^5 \Omega \text{ cm}$, $1.8 \times 10^5 \Omega \text{ cm}$, $2.5 \times 10^5 \Omega \text{ cm}$, and $9.8 \times 10^5 \Omega \text{ cm}$ respectively.

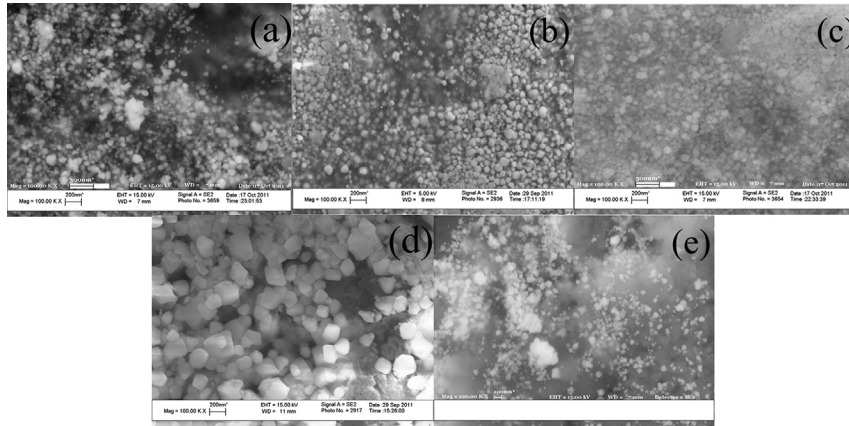


Fig. 3 – Cross Sectional SEM image of the composites that were made of micrometer-sized SDC (HP) Na_2CO_3 1 wt% (a), 5 wt% (b), 10 wt% (c), 20 wt% (d), 50 wt% (e). Each pellet was sintered at 700 °C in air for 1 h.

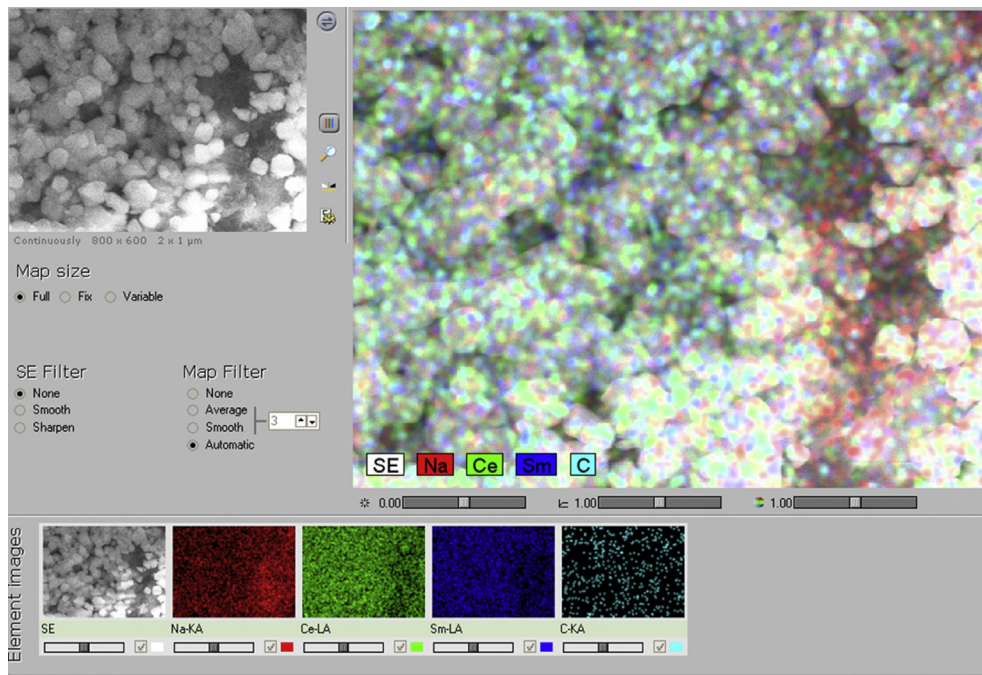


Fig. 4 – Cross Sectional SEM image of the composites that were made of 0.1–0.4 μm size range SDC (HP) Na_2CO_3 20 wt% and EDX micrograph of 20 wt% Na_2CO_3 matrix phase.

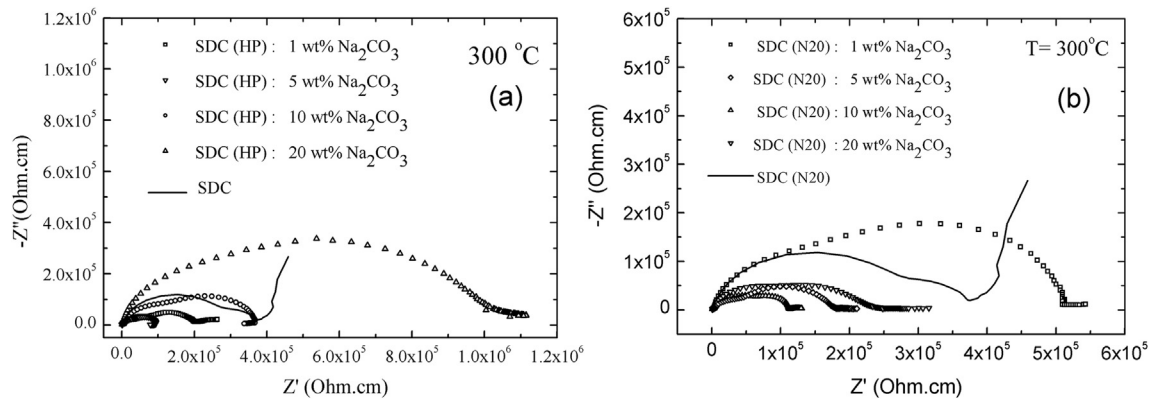


Fig. 5 – The impedance of composites at 300 °C (sintered at 700 °C for 1 h) in which (a) initial composite (SDC HP) contained varied Na_2CO_3 matrix phase and (b) initial composite (SDC N20) contained varied wt % Na_2CO_3 matrix phase.

Discussion

Phase distribution in the SDC- Na_2CO_3 composite

The XRD peaks visible in Fig. 1 all belong to the crystalline SDC. No additional reaction products (new phases) were observed in the XRD patterns of sintered composite pellets. Furthermore, even in composites with up to 75 vol. % (i.e., 50 wt. %) Na_2CO_3 , no strong peaks could be assigned to the Na_2CO_3 matrix phase in the XRD spectra. The absence of diffraction peaks from the carbonate matrix phase could be due to several reasons. The difference between structure factors of the two phases making up the composite is large. The structure factor for x-ray diffraction is closely related to atomic number (Z) of the elements within the phases. While SDC is primarily made up of oxide of heavy cations like Sm ($Z = 62$) and Ce ($Z = 58$), the average Z of Na_2CO_3 is only 14 [24]. Therefore, the possible peaks from the carbonate would have been very weak to be visible next to the strong SDC diffraction intensity. A careful examination of the XRD spectrum of the composite with 50 wt % carbonate reveals very weak diffraction intensity at around 29° which is most likely due to the carbonate matrix phase. At this 50 wt% Na_2CO_3 concentration, the Na_2CO_3 constitutes around 75 volume % of the composite. Thus, the weak peaks from carbonate were observed only in composite with 50 wt% carbonate composition. Another reason for the absence of crystalline peaks may be due to the fact that the carbonate matrix phase is in an amorphous form. In Fig. 1, the x-ray diffraction analysis revealed that the as-received Na_2CO_3 was crystalline and hydrated. The heat-treatment at 700°C caused the monohydrate to lose its water as observed in Fig. 1. Additionally, the ball milling step appeared to have destroyed the crystalline structure of the (bi) carbonate turning it to an amorphous state as mentioned in literature [25]. The study Rojac et al. proved formation of amorphous phase in case of enough milling time intervals [25]. If sufficient ball milling time was provided, 50 wt% Na_2CO_3 composite might transform all its crystalline Na_2CO_3 particles into an amorphous state. However, keeping milling time in constant time interval for all composites to compare the differences in XRD patterns by carbonate ratios in composite. The XRD pattern of composite with 50 wt% carbonate, the peaks of crystalline Na_2CO_3 were detected because of inadequate milling time than composite with 20 wt% carbonate.

The DSC analysis of Na_2CO_3 pellet in Fig. 2 revealed a distinguishable step at 350°C . This feature was assigned to a glass transition of the amorphous Na_2CO_3 phase. No crystalline peaks belonging to Na_2CO_3 in the XRD patterns indicated that a large portion of the carbonate matrix phase in the composite was amorphous with a small portion of crystalline carbonate salt. No chemical reactions lead to a new compound between the SDC and Na_2CO_3 as shown by DSC analyses and XRD patterns. Other studies in the literature also reported an amorphous Na_2CO_3 phase formed after a heat-treatment of SDC and Na_2CO_3 composite [26]. However, just a heat treatment of sodium carbonate did not convert the material into an amorphous structure. It is believed that ball milling SDC particles together with the carbonate salt resulted in partially amorphous carbonate matrix.

The SEM morphology of the composite with 1 wt% Na_2CO_3 (in Fig. 3) showed SDC oxide particles only. The two phases can be differentiated easily by the difference in their image contrast in 50 wt% composite SEM morphology. Two distinct regions can be seen in the SEM micrographs. These regions are the high atomic numbered oxide particles (bright contrast), and the darker carbonate matrix (the glassy and featureless regions) in the composites. In the micrographs that show the EDS elemental maps, the featureless regions were identified as sodium rich carbonate matrix as shown in the composite with 20 wt% carbonate (Fig. 4). On the other hand, the bright contrast regions are the SDC oxides. The SEM micrographs illustrated that the micro-structures of 5 wt% and 10 wt% Na_2CO_3 composites were homogenous (in Fig. 3). The composites were 98% dense. The processing techniques were successful in generating a dense and uniform nano-composite electrolyte as shown in SEM micrographs. On the other hand, even though Na_2CO_3 amount was only 5 wt% (corresponding to 12 vol. %) of the composite, it constituted the matrix phase and glued the oxide particles together during the heat-treatment at 700°C for an hour.

Electrical properties of the SDC- Na_2CO_3 composites

At 300°C , all complex impedance measurements of all samples exhibited in Fig. 5a and b. For the composite prepared with SDC (i.e., HP powders) particles in size range from $0.1\ \mu\text{m}$ to $0.4\ \mu\text{m}$, both the impedance loss ($-Z''$) and the real part of the impedance (Z') values decreased with increasing Na_2CO_3 concentration up to 5 wt%. For instance, the resistivity value for the composite with 1wt% Na_2CO_3 was $1.9 \times 10^5\ (\Omega\ \text{cm})$, for 5 wt% concentration of Na_2CO_3 (~12 vol%) it was on the order of $9.0 \times 10^4\ (\Omega\ \text{cm})$, while the resistivity value in composite with 10 wt% (~24 vol%) Na_2CO_3 was at around $3.8 \times 10^5\ (\Omega\ \text{cm})$ at 300°C . However, when Na_2CO_3 concentration was increased to 20 wt% in the composite, the complex impedance revealed a two overlapped semi-circular arc with a total resistivity value of $1.1 \times 10^6\ (\Omega\ \text{cm})$. The value is higher than the value for 10 wt% Na_2CO_3 containing composite. At all temperatures, Nyquist plots of the composites prepared with SDC (HP) particles containing 5 wt% Na_2CO_3 had the lowest resistivity value.

On the other hand, in the composite prepared with SDC (i.e., N20 powders) in size range from 5 to 10 nm particle, both the impedance loss ($-Z''$) and the real portion of the impedance (Z') values showed a minimum for the Na_2CO_3 concentration of 10 wt%. The resistivity values of both composites with 5 wt % concentration of Na_2CO_3 (~12 vol%), i.e. $1.8 \times 10^5\ (\Omega\ \text{cm})$, and 20 wt% Na_2CO_3 , i.e. $2.5 \times 10^5\ (\Omega\ \text{cm})$, were higher than the one of 10 wt% (~24 vol%) Na_2CO_3 which was $1.2 \times 10^5\ (\Omega\ \text{cm})$ at 300°C . Nyquist plots of the nano-composites prepared with nano-sized particles of SDC (N20) containing 10 wt% Na_2CO_3 showed the lowest resistivity value.

The complex impedance measurements of each composite exhibited two overlapping semi-circular arcs in the Nyquist plots of the composites (shown in Fig. 6a and Fig. 6b). Two semicircles were fitted from original with Z-view program. The deconvolution of the overlapped semicircle indicated that there are at least two chemically distinct components, even without considering interface or grain boundary in between or

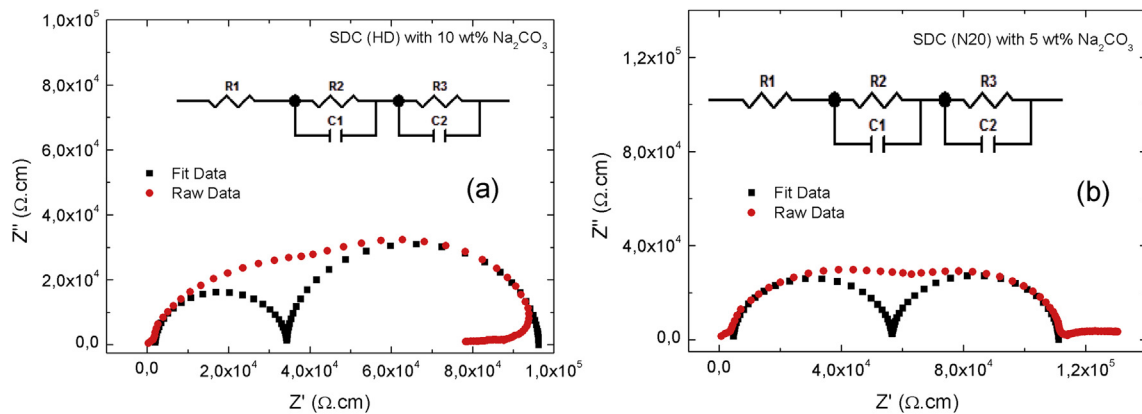


Fig. 6 – Two overlapping semi-circular arcs, shown by Z-View, in the Nyquist plots of the composites. (a) Impedance spectrum and Z-View fitting of the SDC (hp) 10 wt% Na_2CO_3 composite (b) impedance spectrum and Z-View fitting of the SDC (N20) 5 wt% Na_2CO_3 composite.

within them [27]. Two semi-circular arcs with two different relaxation frequencies, calculated from the RC values, such as R_1 , C_1 and R_2 , C_2 , were related to the two different coexisting phases [28,29].

One of the important factors influencing the ionic conductivity of composites was the ratio between Na_2CO_3 and SDC phases. The relative distributions of two phases in the composite were shown in Fig. 6. Below and above an optimum value of relative ratio of two constituent phases, the complex conductivity of composites showed a decrease. This type of percolation behaviour was also observed in other composite systems [20,21]. It appears that the highest conductivity values were obtained in microstructures where both phases, i.e., carbonate matrix phase and the SDC filler phase were interconnected in 3 dimensions. This percolation type behaviour and the unusually high conductivity values for the composite were interpreted as an interface effect in the literature [8,29]. The ionic conductivity values of the composite at 400 °C with various Na_2CO_3 concentrations with two different particle sizes were shown in Fig. 6. For SDC (N20) based Na_2CO_3 composites, the percolation in both phases, shown by fits in Fig. 6a and b, were observed at 10 wt% (~23 vol%) Na_2CO_3 concentrations. On the other hand, the percolation of both phases in the composites with SDC (HP) particles were

observed at 5 wt% (~12 vol%) Na_2CO_3 . Further increase in Na_2CO_3 amount beyond the optimum values in the SDC composites led to a decrease in the total electrical conductivity in both cases.

Another conclusion is the optimum matrix to filler phase ratio was a function of the particle size of filler as illustrated in Fig. 7. The filler oxide, in this case SDC, with the smaller particles sizes and hence the higher surface areas required the higher amounts of the matrix phase for the best conductivity values. It was shown earlier that the interfacial contact area between the constituent phases increased the ionic conductivity [7]. The highest interfacial contact area is possible with the smallest particle size and a uniform structure where both phases are intimately mixed with each other. A continuous interface within the structure is necessary for the so-called “super ionic conduction” [8]. This is only possible if both phases of the composite are connected in the electrolyte structure. As shown in Fig. 7b, by increase of temperature, an increase in conductivity values of each SDC (HP) and SDC (N20) composites were measured. At all temperatures, among the SDC (N20) composites, the composite with 10 wt% Na_2CO_3 had the highest conductivity values. Whereas, for the SDC (HP) composites the one with 5 wt% Na_2CO_3 performed the best conductivity. Furthermore, the ionic conductivity values

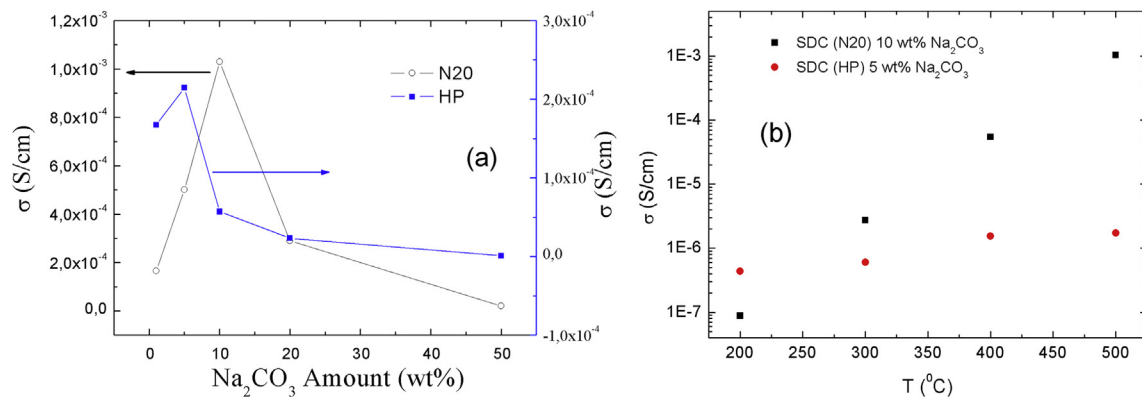


Fig. 7 – The calculate conductivity of the composites at 400 °C. The all composites were containing 5 wt%, 10 wt%, 15 wt%, 20 wt% and 50 wt% of Na_2CO_3 . SDC composite in size range from 5 to 10 nm was labelled as N20 and SDC composite in size range from 0.1 to 0.4 μm was labelled as HP. Composite pellets were heat-treated at 700 °C for 1 h.

of the SDC (N20) composites with 10 wt% Na₂CO₃ was higher than that of SDC (HP) composites with 5 wt% Na₂CO₃.

Conclusion

We presented an approach of designing and developing an ideal amount of Na₂CO₃ phase in SDC composite electrolyte, i.e. a solid equivalent of the “soggy sand” ionic conductors. Varying Na₂CO₃ concentration in the composite electrolyte provided insight into the effect of Na₂CO₃ on the ionic conductivity. Among the several batches of composites prepared with varying amounts of Na₂CO₃, the highest total electrical conductivities were observed for composites with 10 wt% Na₂CO₃ when 5–10 nm size range SDC (N20) oxide filler particles were used. On the other hand, for composite prepared with 0.1–0.4 μm size range SDC (HP) oxide particles, the best carbonate ratio was 5 wt%. The ionic conductivity was dependent on the amount of the interfacial area between the SDC and Na₂CO₃ components.

Acknowledgement

The authors would like to gratefully acknowledge the graduate project support (114M517) by the TÜBİTAK, Turkey. The research leading to these results has received funding from the European Union Seventh Framework Programme under Grant Agreement 312483-ESTEEM2 (Integrated Infrastructure Initiative–I33) via project number 201206-GULGUN.

REFERENCES

- [1] Öncel Ç, Özkaya B, Gülgün MA. X-ray single phase LSGM at 1350 °C. *J Eur Ceram Soc* 2007;27:599.
- [2] Panthi D, Tsutsumi A. Micro-tubular solid oxide fuel cell based on a porous yttria-stabilized zirconia support. *Sci Rep* 2014;4:5754.
- [3] Patakangas J, Ma Y, Jing Y, Lund P. Review and analysis of characterization methods and ionic conductivities for low-temperature solid oxide fuel cells (LT-SOFC). *J Power Sources* 2014;263:315.
- [4] Xia C, Chen F, Liu M. Reduced-temperature solid oxide fuel cells fabricated by screen printing. *Electrochem Solid-State Lett* 2001;4(5):A52–4.
- [5] Wang S, Inaba H, Tagawa H, Dokiya M, Hashimoto T. Nonstoichiometry of Ce_{0.9}Gd_{0.1}O_{1.95–x}. *Solid State Ionics* 1998;107:73.
- [6] Zhu B, Fan L, Lund P. Breakthrough fuel cell technology using ceria-based multi-functional nanocomposites. *Appl Energy* 2013;106:163.
- [7] Shawuti S, Gülgün MA. Solid oxide-molten carbonate nanocomposite fuel cells: Particle size effect. *J Power Source* 2014;267:128.
- [8] Zhu B, Mat MD. Studies on dual phase ceria-based composites in electrochemistry. *Int J Electrochem Sci* 2006;1:383.
- [9] Fan L, Wang C, Chen M, Zhu B. Recent development of ceria-based (nano)composite materials for low temperature ceramic fuel cells and electrolyte-free fuel cells. *J Power Sources* 2013;234:154.
- [10] Wang X, Ma Y, Zhu B. State of the art ceria-carbonate composites (3C) electrolyte for advanced low temperature ceramic fuel cells (LTCFCs). *Int J Hydrogen Energy* 2012;37:19417.
- [11] Fan L, Zhang G, Chen M, Wang C, Di J, Zhu B. Proton and oxygen ionic conductivity of doped ceria-carbonate composite by modified wagner polarization. *Int J Electrochem Sci* 2012;7:8420.
- [12] Fan L, Wang C, Chen M, Di J, Zheng G, Zhu B. Potential low-temperature application and hybrid-ionic conducting property of ceria-carbonate composite electrolytes for solid oxide fuel cells. *Int J Hydrogen Energy* 2011;36:9987.
- [13] Chen M, Zhang H, Fan L, Zhu Bin. Ceria-Carbonate composite for low temperature solid oxide fuel cell: sintering aid and composite effect. *Int J Hydrogen Energy* 2014;39:12309.
- [14] Fan L, Wang C, Di J, Chen M, Zheng J, Zhu B. Study of ceria-carbonate nanocomposite electrolytes for low-temperature solid oxide fuel cells. *J Nanosci Nanotechnol* 2012;12:4941.
- [15] Ferreira ASV, Saradha T, Figueiredo FL, Marques FMB. Compositional and microstructural effects in composite electrolytes for fuel cells. *Int J Energy Res* 2011;35:1090.
- [16] Liu W, Liu Y, Li B, Sparks TD, Wei X, Pan W. Ceria (Sm³⁺, Nd³⁺)/carbonates composite electrolytes with high electrical conductivity at low temperature. *Compos Sci Technol* 2010;70:181.
- [17] Rahman HA, Muchtar A, Muhamad N, Abdullah H. Structure and thermal properties of La_{0.6}Sr_{0.4}Co_{0.2}Fe_{0.8}O_{3–δ} – SDC carbonate composite cathodes for intermediate-to low-temperature solid oxide fuel cells. *Ceram Int* 2012;38:1571.
- [18] Xia C, Li Y, Tian Y, Liu Q, Zhao Y, Jia L, et al. A high performance composite ionic conducting electrolyte for intermediate temperature fuel cell and evidence for ternary ionic conduction. *J Power Sources* 2009;188:156.1.
- [19] Galiński M, Lewandowski A, Stępiak I. Ionic liquids as electrolytes. *Electrochim Acta* 2006;51(26):5567–80.
- [20] Maier J. Space charge regions in solid two-phase systems and their conduction contribution—I. Conductance enhancement in the system ionic conductor-‘inert’ phase and application on AgCl:Al₂O₃ and AgCl:SiO₂. *J Phys Chem Solids* 1985;46:309.
- [21] Bhattacharyya AJ, Mayer J. Second phase effects on the conductivity of non-aqueous salt solutions: “soggy sand electrolytes”. *Adv Mater* 2004;16:811.
- [22] Maier J, Reichert B. Ionic transport in heterogeneously and homogeneously doped thallium (I)-Chloride. *Berichte Bunsenges Für Phys Chem* 1986;90:666.
- [23] Ojovan MI. Viscosity and glass transition in amorphous oxides. *Adv Condens Matter Phys* 2008;817829.
- [24] Yaseda W, Suzuki K. Structure of molten silicon and germanium by X-ray diffraction. *Z Phys B Condens Matter* 1975;20:339.
- [25] Rojac T, Kosec M, Mališ W B, Holc J. The mechanochemical synthesis of NaNbO₃ using different ball-impact energies. *J Am Ceram Soc* 2008;91(5):1559–65.
- [26] Ma Y, Wang X, Raza R, Muhammed M, Zhu B. Thermal stability study of SDC/Na₂CO₃ nanocomposite electrolyte for low-temperature SOFCs. *Int J Hydrogen Energy* 2010;35:2580.
- [27] Barsoukov E, Macdonald JR. Impedance spectroscopy: theory, experiment, and applications. 2nd ed. New Jersey: John Wiley & Sons; 2005. p. 252.
- [28] Pergolesi D, Fabbri E, D’Epifanio A, Di Bartolomeo E, Tebano A, Sanna S, et al. High proton conduction in grain-boundary-free yttrium-doped barium zirconate films grown by pulsed laser deposition. *Nat Mater* 2010;9:846.
- [29] Shawuti S, Can MM, Gülgün MA, Firat T. Grain size dependent comparison of ZnO and ZnGa₂O₄ semiconductors by impedance spectrometry. *Electrochim Acta* 2014;145:132–48.